/ o I
A100466

END
DATE
FILMED
7-81
DTIC

LEVEL II (12)

SECURITY CLASSIFICATION OF THIS PAGE (When Data Entered)

REPORT DOCUMENTATION PAGE	READ INSTRUCTIONS BEFORE COMPLETING FORM	
1. REPORT NUMBER THIRTY-SEVEN	**2. GOVT ACCESSION NO.** AD-A100463	**3. RECIPIENT'S CATALOG NUMBER**
4. TITLE (and Subtitle) Simple and Inexpensive Design for an Isolated Droplet Generator Useful in Studies of Atomization in Flames	**5. TYPE OF REPORT & PERIOD COVERED** Interim Technical Report	
	6. PERFORMING ORG. REPORT NUMBER 45	
7. AUTHOR(s) R. E. Russo, R. Withnell, and G. M. Hieftje	**8. CONTRACT OR GRANT NUMBER(s)** N-14-C-0838 N00014-76-C-0838	
9. PERFORMING ORGANIZATION NAME AND ADDRESS Department of Chemistry Indiana University Bloomington, Indiana 47405	**10. PROGRAM ELEMENT, PROJECT, TASK AREA & WORK UNIT NUMBERS** NR 51-622	
11. CONTROLLING OFFICE NAME AND ADDRESS Office of Naval Research Washington, D.C.	**12. REPORT DATE** June 17, 1981	
	13. NUMBER OF PAGES 20	
14. MONITORING AGENCY NAME & ADDRESS(if different from Controlling Office)	**15. SECURITY CLASS. (of this report)** UNCLASSIFIED	
	15a. DECLASSIFICATION/DOWNGRADING SCHEDULE	

16. DISTRIBUTION STATEMENT (of this Report)

Approved for public release; distribution unlimited

DTIC
ELECTE
JUN 22 1981
E

17. DISTRIBUTION STATEMENT (of the abstract entered in Block 20, if different from Report)

18. SUPPLEMENTARY NOTES

Prepared for publication in APPLIED SPECTROSCOPY

19. KEY WORDS (Continue on reverse side if necessary and identify by block number)

sample introduction   plasma spectrometry
solution dispensing   atomic emission, absorption, fluorescence
droplets
flame spectrometry

20. ABSTRACT (Continue on reverse side if necessary and identify by block number)

A new design is presented for a droplet generator useful in studies of atomization processes in analytical flames. Based in part on medium-scale integrated circuitry, the design is superior in performance to earlier models and is far simpler to construct. Fabrication details are provided and the performance of the new device is assessed.

DD FORM 1473   EDITION OF 1 NOV 65 IS OBSOLETE
1 JAN 73
S/N 0102-014-6601

UNCLASSIFIED

SECURITY CLASSIFICATION OF THIS PAGE (When Data Entered)

81 6 22 104

OFFICE OF NAVAL RESEARCH

Contract ~~N14-76-C-0838~~ $N00014$-76-C-0838

Task No. NR 051-622

TECHNICAL REPORT NO. 37

SIMPLE AND INEXPENSIVE DESIGN FOR AN ISOLATED DROPLET GENERATOR USEFUL IN STUDIES OF ATOMIZATION IN FLAMES

by

R. E. Russo, R. Withnell, and G. M. Hieftje

Prepared for Publication

in

APPLIED SPECTROSCOPY

Indiana University

Department of Chemistry

Bloomington, ~~Indiana~~ 47405

Jun 81

Abstract

A new design is presented for a droplet generator useful in studies of atomization processes in analytical flames. Based in part on medium-scale integrated circuitry, the design is superior in performance to earlier models and is far simpler to construct. Fabrication details are provided and the performance of the new device is assessed.

The authors have for some time been active in the study of fundamental atom formation processes in flames (1-12). In these studies, a droplet generator is employed to produce equally sized spherical droplets of sample solution and to introduce those droplets into an analytical flame with reproducible, isochronal spacing. Initial droplet diameter and spacing must be easily controlled but variable over a wide useful range. With this device, spatial and temporal separation of the individual atom formation processes occurs as a single droplet travels through a flame or plasma. Observation of these processes has then enabled detailed studies to be made on the desolvation of droplets in a flame (1,3,4), vaporization of the resulting solute particles (5,8,10,12), ionization of atoms (12), diffusion of the atoms (8,10), or the velocities of the flame or droplets themselves (6,9,11). Because others have expressed interest in these studies, and in pursuing similar ones, the authors have received numerous requests for circuit and mechanical diagrams of the droplet generator. In the present paper, such information is provided, but for a new system which is much more compact and simpler to construct than earlier versions. The new system achieves high droplet generation stability, enjoys substantial noise immunity in the digital timing network, and can be constructed for under $200. To understand how the new system performs, let us briefly review the nature and function of the droplet generator and how it is employed in the study of atomization mechanisms in flames.

Droplet Generator Mechanical System and Operation

The droplet generator system for analytical atomic spectrometry was originally described in the literature several years ago (1,2). Therefore, its operation is only briefly described herein. The components of the droplet generator are displayed in Figure 1, which was adapted from the original figure in reference 1.

In operation, droplets are generated by launching a periodic mechanical disturbance onto the surface of a jet of sample solution. In turn, the jet is formed by forcing the desired solution through a capillary fabricated from borosilicate glass (1mm, i.d.). Ordinarily, the tip of the capillary is constricted by fire polishing to approximately 25 μm in diameter, although other orifice diameters can be employed for the generation of larger or smaller droplets. A Millipore filter placed between the solution reservoir and the capillary prevents blocking by foreign materials suspended in the solution.

To generate the mechanical disturbance, the capillary is mounted in a cantilever fashion to a bimorph electromechanical transducer (PZT-5H, Vernitron Company, Bedford, OH). Applying an alternating voltage to the bimorph causes it to vibrate, breaking the stream up into well-defined droplets. The number of droplets which are generated per unit time is equal to the mechanical frequency and therefore to that of the oscillator driver (Hewlett Packard, Model 200CDR); in our work, this value ranges between 10,000 and 60,000 droplets per second.

To select individual droplets, the liquid jet is surrounded by a brass ring at the point where droplets detach from the jet. A medium-voltage pulse of positive polarity (50-300 V) applied to this

ring repels charges in the liquid jet, causing the end of the jet to become slightly negative. A droplet detaching from the jet at this moment captures the negative charge, so that it can be electrostatically deflected. Passage of the entire droplet stream between two plates charged to opposite polarity voltages then extracts the charged droplets from the stream, enabling them to be sent reproducibily into a flame. Because the number of droplets which are charged per unit time can be adjusted, droplets can be introduced into the flame at rates from less than one droplet per minute to as high as the driving frequency of the bimorph. Uncharged droplets are captured by a glass trap and directed to a drain. With the system discussed in this paper, it is also possible to trap charged droplets and enable uncharged droplets to travel into the flame, simply by reversing the polarity of the high-voltage plates.

For reproducibility in the charging of droplets and thereby in their selection, it is important to synchronize each charging pulse with the droplet generation process. Accordingly, the charging rate is ordinarily a submultiple of the droplet generation frequency and is adjusted by means of a frequency divider. Selection of the time for application of the charging pulse is controlled by means of a suitable delay circuit, to be discussed later.

A photograph showing the droplet generation system in operation is reproduced in Figure 2. In this figure, a single high-intensity flash from a stroboscopic source shows droplets being introduced into a flame at a rate of approximately 1300 droplets per second. However, because of the stability of the droplet generator and the flame, the photograph could also represent the sequential changes which occur to

a single droplet as it travels through the flame. Even visually, one can observe the decrease in droplet size as it desolvates and the emitting plume of atoms which are liberated during vaporization of a single solute particle. Clearly, to provide the spatial and temporal separation of these events which are obserable in Figure 2 requires a droplet generation system which is highly precise and stable.

New Droplet Generator System

A block diagram of the new analog and digital electronic circuits used in the droplet generator is shown in Figure 3. These circuits were designed to produce accurate division of the oscillator frequency and a reproducible pulse duration and amplitude for charging individual droplets. A digital frequency meter was incorporated into the system to indicate either the bimorph driving frequency or the droplet charging rate, whichever is desired. In addition, a pulse amplitude meter was installed to indicate the voltage level applied to the charging ring. In Figure 3, the pulse which is ultimately used to charge those droplets to be deflected is produced in synchronism with the oscillator (OSC) which drives the piezoelectric bimorph. Synchronism is accomplished by dividing the oscillator frequency by a value which is set by front-panel binary switches (BS). After frequency division, the divider produces a narrow pulse for every N cycles of the driving oscillator, where N is the number set on the front panel. A selectable delay then enables the pulse to be positioned accurately with respect to droplet production, to yield the greatest charge on each droplet. Similarly, the width of the charging

pulse can be adjusted by a subsequent device so that only one droplet at a time is charged. Finally, an adjustable-gain amplifier, driven by a high-voltage power supply (PS) produces a delayed, adjustable-width pulse of the proper voltage. A detailed circuit diagram for each of these blocks is discussed in the following sections.

Digital Frequency Divider, Pulse Delay, and Pulse Width Network

The function of this network is to regulate the number of droplets which are charged and to charge those droplets optimally so they can be removed most effictively from the main droplet stream. Specific requirements to be met are that the pulses occur at a preset submultiple of the capillary driving frequency and with reproducible amplitude and width. In addition, the pulse width and temporal spacing must be variable so it can be positioned to yield the maximum charge on a droplet as it detaches from the liquid jet. A diagram of the new electronic system which satisfies these requirements is shown in Figure 4. Standard TTL positive logic levels have been used throughout.

Section S-1 shapes the input sine wave from the oscillator into a square wave. The input sine wave is "clipped" by the combination of resistor R1 and diode D1, so only positive voltage levels appear at the base of transistor T1. Transistor T1 serves merely as a binary switch whose output is further shaped and rendered TTL compatible by a 7414 Schmitt trigger. This squared synchronizing waveform is then sent through a variable-modulus counter which serves as a frequency divider. The variable-modulus frequency divider is constructed from

integrated circuit counters (7493) and a binary-switch reset network. The center tap of each of the binary switches is connected to the inputs of NAND gates G1 and G2. When all binary switches are in the down position (the center terminal connected to the top 4.4 V terminal), a logical "1" is connected to each input of NAND gates G1 and G2. After inversion by G3 and G4, this situation produces an output of logical "0" from gate G5 which prevents delay monostable M1 from triggering. Consequently, no output pulse is produced. When any binary switch is moved to the up position, the corresponding output of the variable modulus counter is connected to the input of G1 or G2. Initially, all outputs of the counter are low (cleared) so the output of G5 goes high, readying the delay monostable M1 for triggering (negative edge trigger). At this time, the Q output of M1 is low. When the binary counter reaches the number of counts specified by the activated switches, all inputs to G1 and G2 are again high, causing G5 to go low and trigger M1.

Two events occur simultaneously when M1 triggers: $\overline{Q}$ of M1 goes low triggering the reset monostable M3, and Q of M1 goes high readying the pulse width monostable M2 for triggering. The counter is immediately cleared so that no counts from the oscillator are lost. After the selected delay of M1 (determined by a variable resistor-capacitor network on the front panel), Q of M1 goes low, triggering M2, and thereby generating a digital output pulse. The duration of this pulse is also controlled by a resistor-capacitor arrangement on the front panel. The precision in the pulse width was measured to be approximately 0.1%, in agreement with specifications of the 74221 monostable. Monostable M4 is used as a synchronizing output

pulse and triggers each time $\overline{Q}$ of M1 goes low. The output of M4 is connected to a BNC connector on the front panel and is sent to a triggered stroboscope used for observation of the charged droplets.

Section S-2 is employed to inform the operator if delay monostable M1 is set so long that output pulses might be lost. Such a situation would occur if the selected delay is greater than the pulse spacing. Once M1 has triggered (Q goes high), it cannot respond to another trigger pulse from G5. Therefore, if Q of M1 is high and G5 goes low (G6 goes high), a default condition has occurred. In this event, G7 goes low, triggering monostable M5 which lights an LED on the front panel. The Si diode, 220 Ω resistor and 0.015 μf capacitor are used for timing the pulse arrival at G7, ensuring that the LED will light only when delay overlap occurs.

Frequency Meter A circuit diagram for the frequency meter used in the present instrument is shown in Figure 5A; a timing diagram indicating the sequence of events in the frequency meter is drawn in Figure 5B. Monostables M1 and M2 form an astable multivibrator which controls the switching and counting of the frequency meter. Pull-up resistors (22 KΩ) and coupling capacitors (0.001 μf) are used between M1 and M2 to ensure correct logic-level crossings.

A binary switch on the front panel determines whether the bimorph oscillator frequency or droplet charging pulse frequency is applied to the clock input of the 74C925 counter/multiplexer (National Semiconductor, MM74C925). The 74C925 counter is a multifunctional component, and serves as both a four-digit counter and multiplexed seven-segment display driver. The four seven-segment displays are

connected in parallel so only seven 50 ohm resistors are required to drive the entire array. The multiplexer separately accesses each of the displays by forward-biasing the appropriate transistor. The multiplexer cycle frequency is 1 KHz; therefore, a number stored in the data latch visually appears to be flicker-free and displayed continuously. The clock in the 74C925 is allowed to count for one second (determined by M1). At the end of this time, M3 applies a short (50 µs) pulse to latch the count into memory, and it is immediately displayed. After the latch pulse, a short (50 µs) reset pulse from monostable M4 clears the counter. The end of the reset pulse also signals the beginning of the count cycle (M4 could be connected directly to the trigger of M1). A particular count remains in the data latch (and is displayed) even though the clear (reset) pulse is issued; only a new latch pulse can change the display. Therefore, the display is continuous and updated every second. The frequency meter was calibrated with a separate digital meter (Model 5302A Universal Counter, Hewlett Packard, Palo Alto, CA) and stable oscillator (Digital Timing Module, Heath Company, Benton Harbor, MI) The timing of M1 is adjusted using a variable resistor to compensate for switching times and exact pulse times (from nominal values). The precision and accuracy of the frequency meter designed here were measured to be 0.1%.

Analog High-Voltage Power Supply The requirement of the analog section is to deliver a high-voltage (0-250 V), fast rise-time pulse for the time period (10-60 µs) commanded by the digital pulse-forming network. The new circuit design for this application is shown in

Figure 6. The components to the left of the dashed line form a variable high-voltage power supply; the components to the right form the high-voltage pulsing network. In the high-voltage power section, a capacitively filtered full-wave rectifier supplies 280 V to pass transistor T1 whose resistance controls the output voltage for the charging ring. The resistance of T1 is varied by amplifier A and control transistor T2 through a front panel variable resistor R2. Specifically, the inverting input of A will be held at approximately the same voltage as V1, which is controlled by the external resistor network R2 and R3. To maintain this balance, amplifier A will adjust the current to T2, varying its effective resistance. In turn, the base current to pass transistor T1 and thereby the output voltage V2 is determined by the effective resistance of T2. The particular output voltage level is displayed on a pulse amplitude meter on the front panel. The two diodes (1N4002) are placed between the inputs of amplifier A to protect it from excessively high voltage (such as when the front panel assembly is disconnected).

The pulsing section is designed to pass the voltage level at V2 to the output charging ring upon command from the digital network. As discussed above, the voltage level at V2 is set by the pulse amplitude control on the front panel. The logic pulse from the digital divider network (cf., Figures 4 and 5) is applied to the base of T4, controlling its bias. When the input level to the base of T4 is high, V5 is near 0 V. Therefore, transistor T3 passes the high voltage at V2 to the output (charging ring). When the base of T4 is low, V5 is at +15 V and T3 is off, inhibiting the output. The pulsing rate follows the input logic frequency. The pulse characteristics

(switching times) are determined by the PN junction capacitance of T3 and resistor R6. Specifically, the rise time is governed primarily by the switching (ON) time of transistor T3 and was measured as 420 ns. The fall time is determined by the switching (CFF) time of T3 and resistor R6, and measured to be 12 μs.

A photograph of the new droplet generator front panel shown in Figure 8 reveals the position of the controls which has been found to be most convenient.

Critique

The new droplet generator electronics provide accurate and precise charging pulses with reproducible amplitude and width. The digital electronic circuits are completely shielded from the analog high-voltage circuits, eliminating noise problems which existed in earlier models. Rapidly rising and falling digital pulses are available at variable rates from one pulse per minute to several thousand pulses per second. The output of the analog high-voltage section can be varied from 0-250 V, and is stable at each selected level. The analog switching network exhibits very fast rise and fall times with no voltage over-shoot, so no pulse overlap exists; consequently, single droplets can be charged with no effect on preceding or succeeding droplets. In addition, the analog switching section can be connected to a separate regulated high-voltage supply (13) and still provide the same pulse characteristics. Droplets produced using the new electronic system were also found to exhibit excellent spatial and temporal stability.

(switching times) are determined by the PN junction capacitance of T3 and resistor R6. Specifically, the rise time is governed primarily by the switching (ON) time of transistor T3 and was measured as 420 ns. The fall time is determined by the switching (OFF) time of T3 and resistor R6, and measured to be 12 μs.

A photograph of the new droplet generator front panel shown in Figure 8 reveals the position of the controls which has been found to be most convenient.

Critique

The new droplet generator electronics provide accurate and precise charging pulses with reproducible amplitude and width. The digital electronic circuits are completely shielded from the analog high-voltage circuits, eliminating noise problems which existed in earlier models. Rapidly rising and falling digital pulses are available at variable rates from one pulse per minute to several thousand pulses per second. The output of the analog high-voltage section can be varied from 0-250 V, and is stable at each selected level. The analog switching network exhibits very fast rise and fall times with no voltage over-shoot, so no pulse overlap exists; consequently, single droplets can be charged with no effect on preceding or succeeding droplets. In addition, the analog switching section can be connected to a separate regulated high-voltage supply (13) and still provide the same pulse characteristics. Droplets produced using the new electronic system were also found to exhibit excellent spatial and temporal stability.

Literature Cited

1. G. M. Hieftje and H. V. Malmstadt, Anal. Chem., 40, 1860 (1968).

2. G. M. Hieftje and H. V. Malmstadt, Anal. Chem., 41, 1735 (1969).

3. N. C. Clampitt and G. M. Hieftje, Anal. Chem., 44, 1211 (1972).

4. N. C. Clampitt and G. M. Hieftje, Anal. Chem., 46, 382 (1974).

5. G. J. Bestiaans and G. M. Hieftje, Anal. Chem., 46, 901 (1974).

6. C. B. Boss and G. M. Hieftje, Anal. Chem., 49, 2112 (1977).

7. C. B. Boss and G. M. Hieftje, Appl. Spectrosc., 32, 377 (1978).

8. C. B. Boss and G. M. Hieftje, Anal. Chem., 51, 895 (1979).

9. R. E. Russo and G. M. Hieftje, Anal. Chim. Acta, 118, 293 (1980).

10. C. B. Boss and G. M. Hieftje, Anal. Chem., 51, 1897 (1979).

11. R. E. Russo and G. M. Hieftje, Spectrochim. Acta, Part B, 36, 231 (1981).

12. B. D. Bleasdell, E. P. Wittig and G. M. Hieftje, Spectrochim. Acta, Part B, 36, 205 (1981).

13. R. E. Lemke, Masters Thesis, Indiana University, 1980.

Figure Captions

Figure 1. Schematic diagram of the droplet generator.

Figure 2. Photograph of droplets injected into an air-acetylene flame at a rate of approximately 1300 droplets per second.
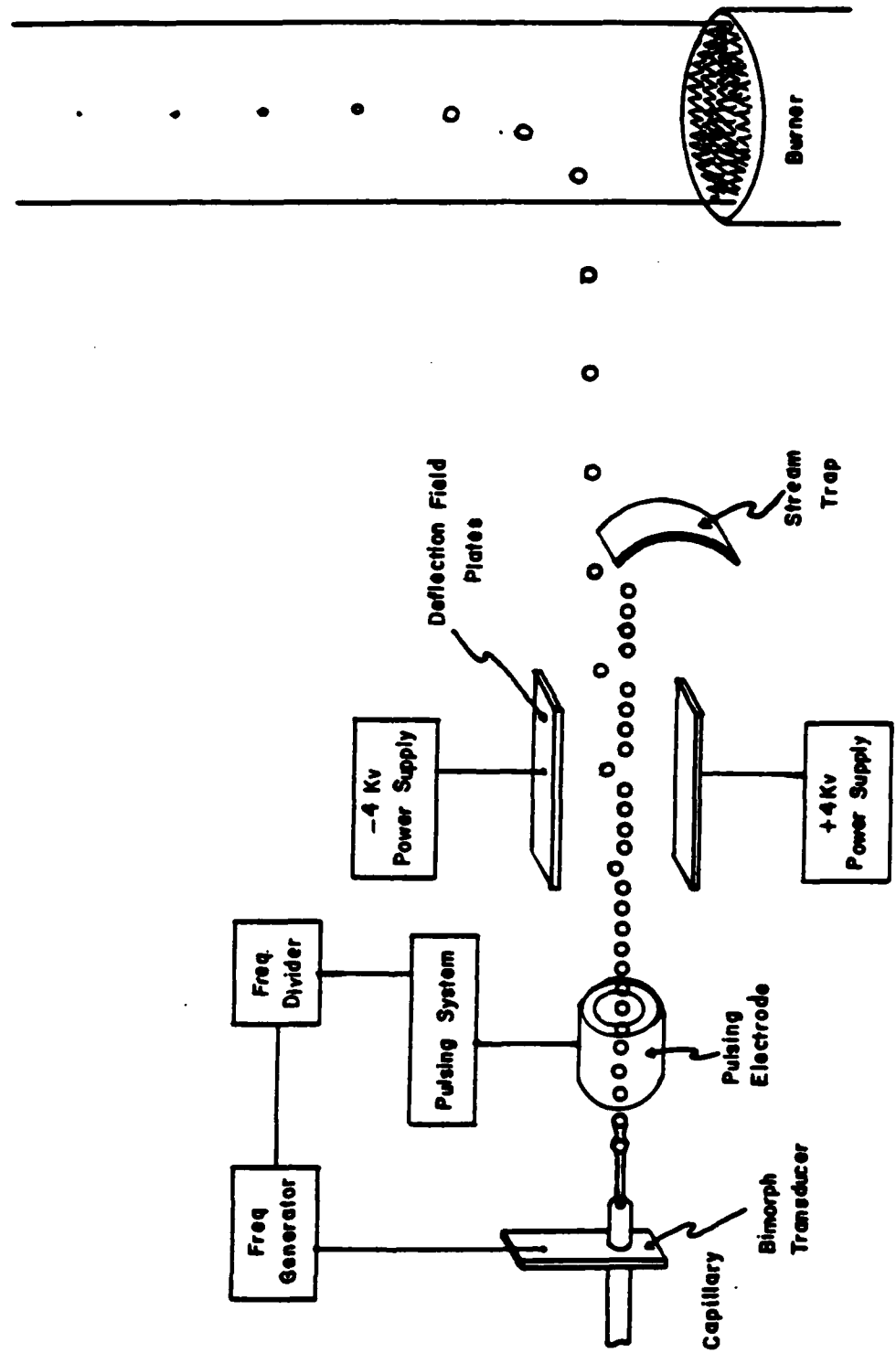
Figure 3. Block diagram of the electronic control section for the droplet generator. PS, power supply; OSC, oscillator; and BS, binary switches.
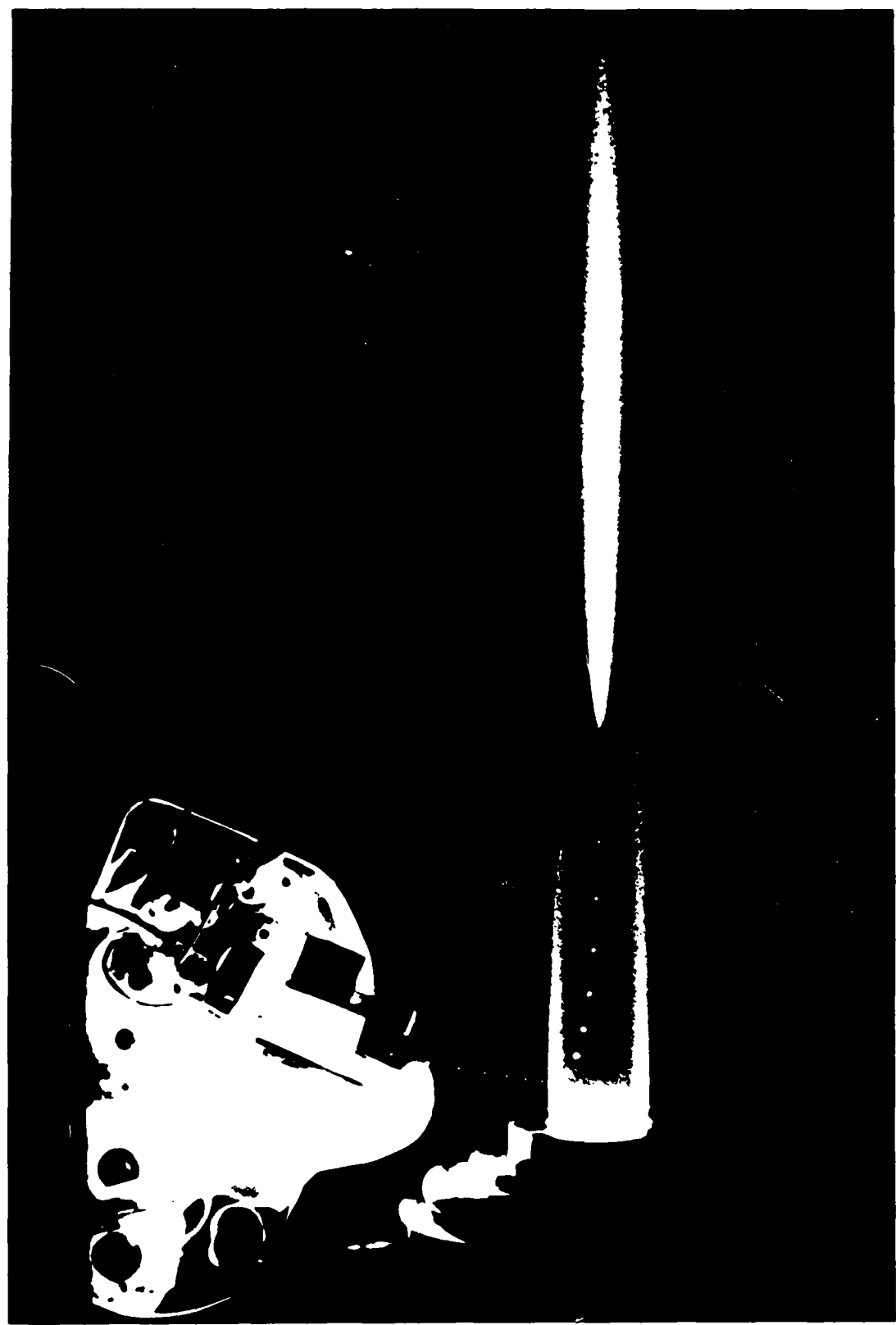
Figure 4. Circuit diagram of the digital frequency divider network for the new droplet generator.
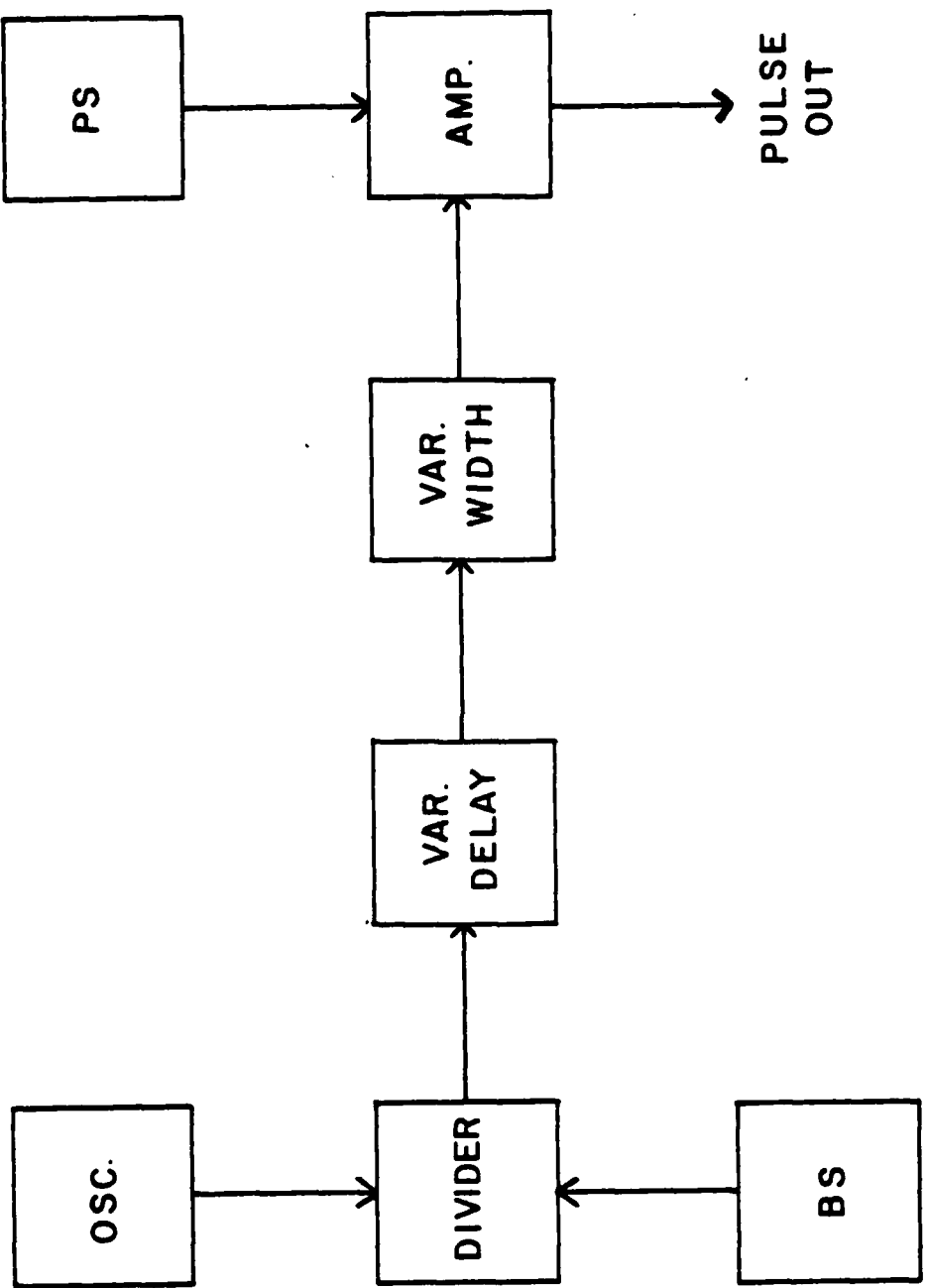
Figure 5. Digital frequency meter. A, diagram of circuit; B, timing diagram defining sequence of events.
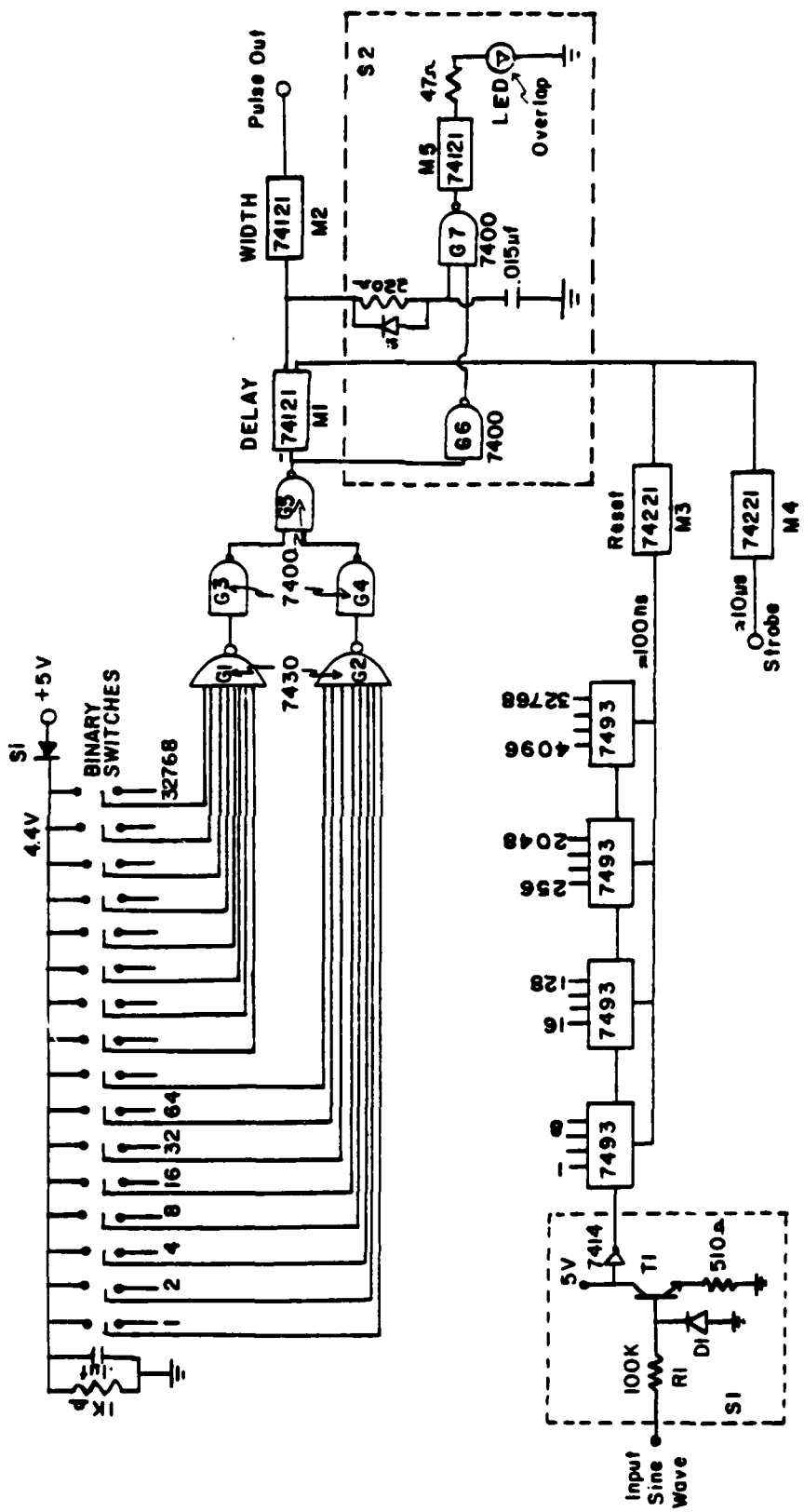
Figure 6. Circuit diagram of analog high-voltage and switching network for pulsing electrode signal. D1 and D2 are 1N4002 diodes.
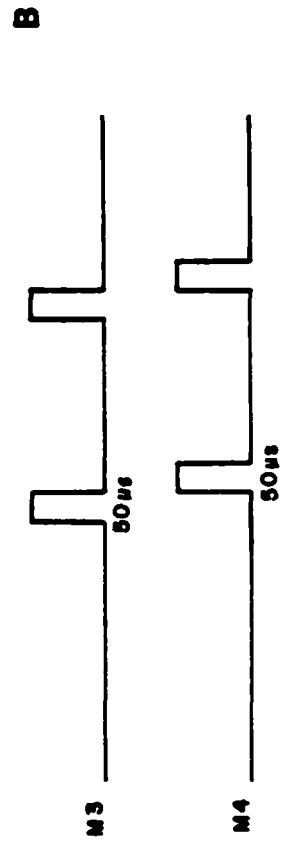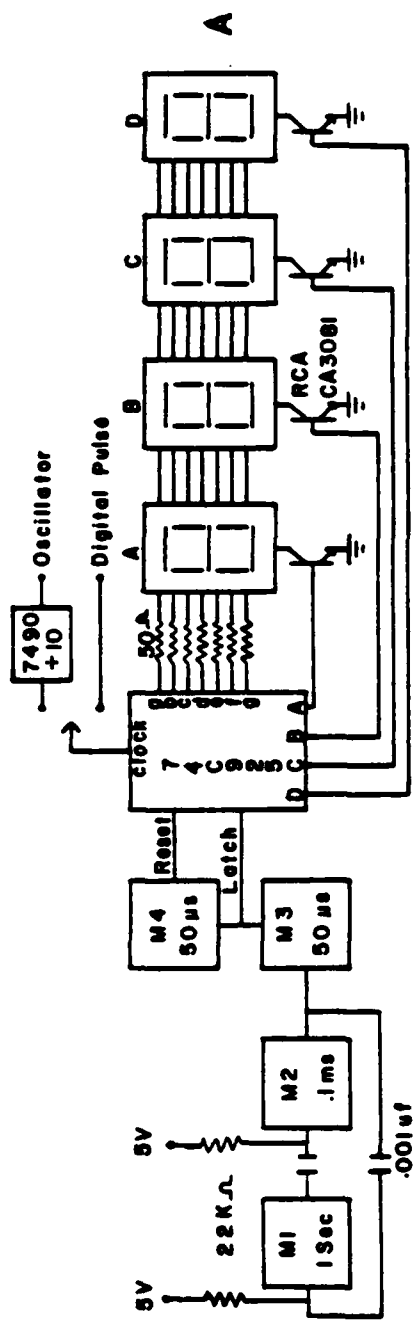
Figure 7. Photograph of the droplet generator controller front panel.

Burner

Deflection Field Plates

Stream Trap

−4 Kv Power Supply

+4 Kv Power Supply

Freq. Divider

Pulsing System

Pulsing Electrode

Freq. Generator

Bimorph Transducer

Capillary

Oscillator

7490 +10

Digital Pulse

A B C D

RCA CA3081

50Ω

Clock
7 4 C 9 5
D C B A

Reset

Latch

M4 50µs

M3 50µs

M2 .1ms

M1 1Sec

5V

5V

22KΩ

.001µf

A

B

M1

1S

M2

.1ms

M3

50µs

M4

50µs
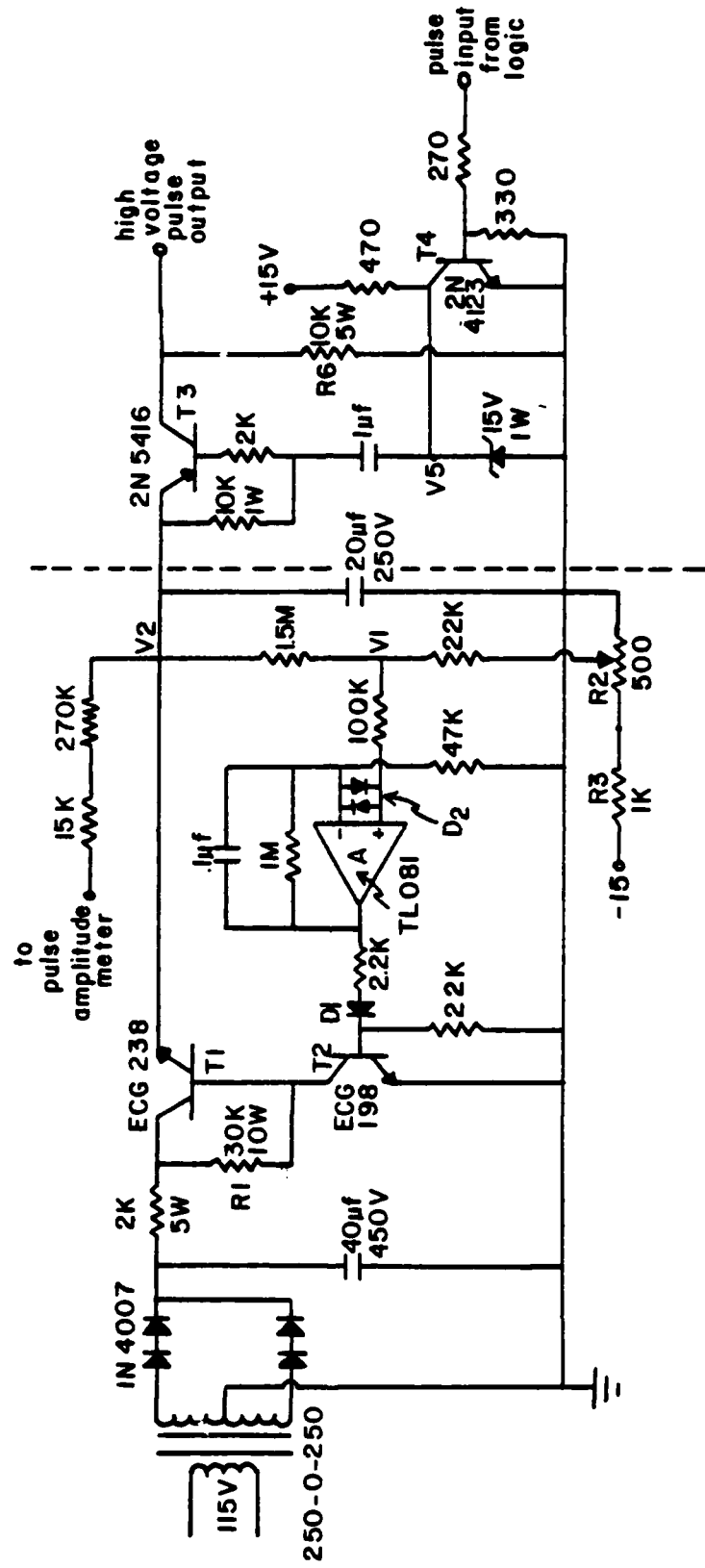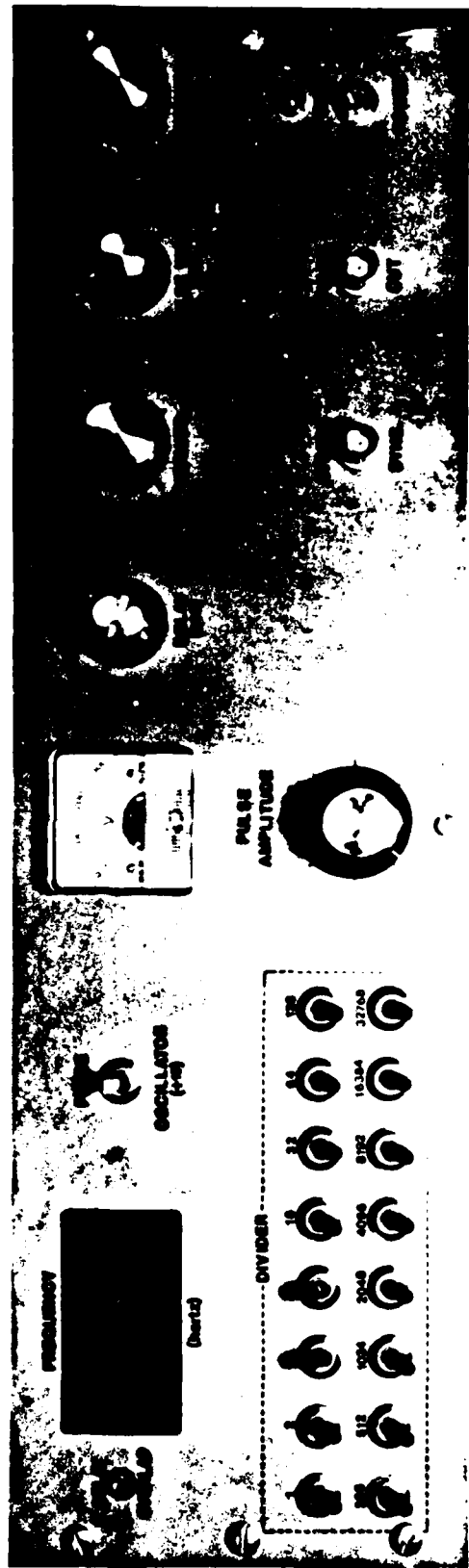
TECHNICAL REPORT DISTRIBUTION LIST, GEN

	No. Copies		No. Copies
Office of Naval Research Attn: Code 472 800 North Quincy Street Arlington, Virginia 22217	2	U.S. Army Research Office Attn: CRD-AA-IP P.O. Box 1211 Research Triangle Park, N.C. 27709	1
ONR Branch Office Attn: Dr. George Sandoz 536 S. Clark Street Chicago, Illinois 60605	1	Naval Ocean Systems Center Attn: Mr. Joe McCartney San Diego, California 92152	1
ONR Area Office Attn: Scientific Dept. 715 Broadway New York, New York 10003	1	Naval Weapons Center Attn: Dr. A. B. Amster, Chemistry Division China Lake, California 93555	1
ONR Western Regional Office 1030 East Green Street Pasadena, California 91106	1	Naval Civil Engineering Laboratory Attn: Dr. R. W. Drisko Port Hueneme, California 93401	1
ONR Eastern/Central Regional Office Attn: Dr. L. H. Peebles Building 114, Section D 666 Summer Street Boston, Massachusetts 02210	1	Department of Physics & Chemistry Naval Postgraduate School Monterey, California 93940	1
Director, Naval Research Laboratory Attn: Code 6100 Washington, D.C. 20390	1	Dr. A. L. Slafkosky Scientific Advisor Commandant of the Marine Corps (Code RD-1) Washington, D.C. 20380	1
The Assistant Secretary of the Navy (RE&S) Department of the Navy Room 4E736, Pentagon Washington, D.C. 20350	1	Office of Naval Research Attn: Dr. Richard S. Miller 800 N. Quincy Street Arlington, Virginia 22217	1

Commander, Naval Air Systems Command
Attn: Code 310C (H. Rosenwasser)
Department of the Navy
Washington, D.C. 20360
	1	Naval Ship Research and Development
		  Center
		Attn: Dr. G. Bosmajian, Applied
		  Chemistry Division
		Annapolis, Maryland 21401
			1

Defense Technical Information Center Building 5, Cameron Station Alexandria, Virginia 22314	12	Naval Ocean Systems Center Attn: Dr. S. Yamamoto, Marine Sciences Division San Diego, California 91232	1
Dr. Fred Saalfeld Chemistry Division, Code 6100 Naval Research Laboratory Washington, D.C. 20375	1	Mr. John Boyle Materials Branch Naval Ship Engineering Center Philadelphia, Pennsylvania 19112	1

TECHNICAL REPORT DISTRIBUTION LIST, 051C

	No. Copies		No. Copies
Dr. M. B. Denton Department of Chemistry University of Arizona Tucson, Arizona 85721	1	Dr. John Duffin United States Naval Postgraduate School Monterey, California 93940	1
Dr. R. A. Osteryoung Department of Chemistry State University of New York at Buffalo Buffalo, New York 14214	1	~~Dr. G. M. Hieftje~~ ~~Department of Chemistry~~ ~~Indiana University~~ ~~Bloomington, Indiana 47401~~	1
Dr. B. R. Kowalski Department of Chemistry University of Washington Seattle, Washington 98105	1	Dr. Victor L. Rehn Naval Weapons Center Code 3813 China Lake, California 93555	1
Dr. S. P. Perone Department of Chemistry Purdue University Lafayette, Indiana 47907	1	Dr. Christie G. Enke Michigan State University Department of Chemistry East Lansing, Michigan 48824	1
Dr. D. L. Venezky Naval Research Laboratory Code 6130 Washington, D.C. 20375	1	Dr. Kent Eisentraut, MBT Air Force Materials Laboratory Wright-Patterson AFB, Ohio 45433	1
Dr. H. Freiser Department of Chemistry University of Arizona Tuscon, Arizona 85721		Walter G. Cox, Code 3632 Naval Underwater Systems Center Building 148 Newport, Rhode Island 02840	1
Dr. Fred Saalfeld Naval Research Laboratory Code 6110 Washington, D.C. 20375	1	Professor Isiah M. Warner Texas A&M University Department of Chemistry College Station, Texas 77840	1
Dr. H. Chernoff Department of Mathematics Massachusetts Institute of Technology Cambridge, Massachusetts 02139	1	Professor George H. Morrison Cornell University Department of Chemisty Ithaca, New York 14853	1
Dr. K. Wilson Department of Chemistry University of California, San Diego La Jolla, California	1	Dr. Rudolph J. Marcus Office of Naval Research Scientific Liaison Group American Embassy APO San Francisco 96503	1
Dr. A. Zirino Naval Undersea Center San Diego, California 92132	1	Mr. James Kelley DTNSRDC Code 2803 Annapolis, Maryland 21402	1